bioRxiv preprint doi: https://doi.org/10.1101/2020.09.24.311654; this version posted September 25, 2020. The copyright holder for this preprint (which was not certified by peer review) is the author/funder. All rights reserved. No reuse allowed without permission.

Title

Associations between ADHD symptom remission and white matter microstructure: a longitudinal analysis

Running title

ADHD symptom remission and white matter

Authors

Anne E. M. Leenders, M.Sc.[1*], Christienne G. Damatac, M.Sc.[1,2*], Sourena Soheili-Nezhad, M.D.[1,2], Roselyne J. M. Chauvin, Ph.D.[1,2], Maarten J. J. Mennes, Ph.D.[1,2], Marcel P. Zwiers, Ph.D.[1,2], Daan van Rooij, Ph.D.[1,2], Sophie E. A. Akkermans, Ph.D.[1,3], Jilly Naaijen, Ph.D.[1,2], Barbara Franke, Ph.D.[3,4], Jan K. Buitelaar, Ph.D.[1,2,5], Christian F. Beckmann, PhD[1,2,6], Emma Sprooten, PhD[1,2]

Affiliations

1. Centre for Cognitive Neuroimaging, Donders Institute for Brain, Cognition and Behaviour, Radboud University, Nijmegen, the Netherlands.
2. Department of Cognitive Neuroscience, Donders Institute for Brain, Cognition and Behaviour, Radboud University Medical Centre, Nijmegen, the Netherlands.
3. Department of Human Genetics, Donders Institute for Brain, Cognition and Behaviour, Radboud University Medical Centre, Nijmegen, the Netherlands
4. Department of Psychiatry, Donders Institute for Brain, Cognition and Behaviour, Radboud University, Nijmegen, the Netherlands
5. Karakter Child and Adolescent Psychiatry University Centre, Nijmegen, the Netherlands
6. Centre for Functional MRI of the Brain, University of Oxford, Oxford, UK

* These authors contributed equally to this work.

bioRxiv preprint doi: https://doi.org/10.1101/2020.09.24.311654; this version posted September 25, 2020. The copyright holder for this preprint (which was not certified by peer review) is the author/funder. All rights reserved. No reuse allowed without permission.

Corresponding author

Correspondence to Christienne G. Damatac, Department of Cognitive Neuroscience, Donders Centre for Cognition, Donders Institute for Brain, Cognition and Behaviour, Kapittelweg 29, 6525 EN Nijmegen, The Netherlands; c.gonzalesdamatac@donders.ru.nl

Funding, acknowledgments, and financial disclosures

The NeuroIMAGE study was supported by NIH Grant R01MH62873 (to Stephen V. Faraone), NWO Large Investment Grant 1750102007010 (to Jan Buitelaar), ZonMW grant 60-60600-97- 193, NWO grants 056-13-015 and 433-09-242, and matching grants from Radboud University Nijmegen Medical Center, University Medical Center Groningen and Accare, and Vrije Universiteit Amsterdam.

A.E.M.L. reports no biomedical financial interests or potential conflicts of interest.

C.G.D. reports no biomedical financial interests or potential conflicts of interest.

S.S.N. reports no biomedical financial interests or potential conflicts of interest.

R.J.M.C. reports no biomedical financial interests or potential conflicts of interest.

M.J.J.M. reports no biomedical financial interests or potential conflicts of interest.

M.P.Z. reports no biomedical financial interests or potential conflicts of interest.

D.v.R reports no biomedical financial interests or potential conflicts of interest.

S.E.A.A. reports no biomedical financial interests or potential conflicts of interest.

J.N. is funded by a personal Veni grant from the Innovation Program of the Netherlands Organization for Scientific Research (NWO; grant VI.Veni.194.032).

B.F. has received support from the European Community's Horizon 2020 Programme (H2020/2014 – 2020) under grant agreement n° 667302 (CoCA) and has received educational speaking fees from Medice.

J.K.B. has been consultant to/member of advisory board of and/or speaker for Janssen Cilag BV, Eli Lilly, Bristol-Myer Squibb, Shering Plough, UCB, Shire, Novartis and Servier. He is

bioRxiv preprint doi: https://doi.org/10.1101/2020.09.24.311654; this version posted September 25, 2020. The copyright holder for this preprint (which was not certified by peer review) is the author/funder. All rights reserved. No reuse allowed without permission.

not an employee of any of these companies, nor a stock shareholder of any of these companies.

C.F.B. reports no biomedical financial interests or potential conflicts of interest.

E.S. is funded by a Hypatia Fellowship (Radboudumc) and a NARSAD Young Investigator Grant (Brain and Behavior Research Foundation, ID: 25034).

Key words

1. ADHD
2. white matter microstructure
3. diffusion weighted imaging
4. remission
5. longitudinal

Main body of text: 3,737 words

bioRxiv preprint doi: https://doi.org/10.1101/2020.09.24.311654; this version posted September 25, 2020. The copyright holder for this preprint (which was not certified by peer review) is the author/funder. All rights reserved. No reuse allowed without permission.

Abstract

Objective

Attention-deficit hyperactivity disorder (ADHD) is associated with white matter (WM) microstructure. Our objective was to investigate how WM microstructure is longitudinally related to symptom remission in adolescents and young adults with ADHD.

Method

We obtained diffusion-weighted imaging (DWI) data from 99 participants at two time points (mean age baseline: 16.91 years, mean age follow-up: 20.57 years). We used voxel-wise Tract-Based Spatial Statistics (TBSS) with permutation-based inference to investigate associations of inattention (IA) and hyperactivity-impulsivity (HI) symptom change with fractional anisotropy (FA) at baseline, follow-up, and change difference between time points.

Results

Remission of combined HI and IA symptoms was significantly associated with reduced FA at follow-up in the left superior longitudinal fasciculus and the left corticospinal tract (CST) (P_{FWE}=0.038 and P_{FWE}=0.044, respectively), mainly driven by an association between HI remission and follow-up CST FA (P_{FWE}=0.049). There was no significant association of combined symptom remission with FA at baseline or with changes in FA between the two assessments.

Conclusion

In this longitudinal DWI study of ADHD using dimensional symptom scores, we show that greater symptom remission is associated with lower follow-up FA in specific WM tracts. Altered FA thus may appear to follow, rather than precede, changes in symptom remission. Our findings indicate divergent WM developmental trajectories between individuals with persistent and remittent ADHD, and support the role of prefrontal and sensorimotor tracts in the remission of ADHD.

bioRxiv preprint doi: https://doi.org/10.1101/2020.09.24.311654; this version posted September 25, 2020. The copyright holder for this preprint (which was not certified by peer review) is the author/funder. All rights reserved. No reuse allowed without permission.

Introduction

Attention-deficit/hyperactivity disorder (ADHD) is a common neuropsychiatric disorder characterized by developmentally inappropriate levels of inattention (IA) and/or hyperactivity-impulsivity (HI), with an estimated prevalence of 5% in children and adolescents and 2.5% in adults.[1] For many, ADHD begins in childhood, but the long-term clinical course of ADHD varies widely between individuals.[2] Prospective studies suggest that although only 15% of children with ADHD continue to fully meet diagnostic criteria in adulthood, 60-70% of them retain impairing symptoms in adulthood.[1] ADHD diagnosis has been associated with altered patterns of brain structure and function, however the neural mechanisms related to symptom progression (i.e. remission vs. persistence) have not yet been fully unravelled.[3–7] Understanding this could help develop and tailor treatments to benefit long-term outcomes for children with ADHD.

The underlying neural mechanisms that drive symptom remission may be distinct from those that drive ADHD onset, thus the brains of remitted individuals could be methodologically differentiated from those of people who were never diagnosed with ADHD.[8] Here, we refer to symptom remission as a dimensional concept, as a decrease in symptom severity between two time-points. Symptom remission can be driven by a number of neurodevelopmental mechanisms which are not mutually exclusive. Previous hypotheses suggest that disorder onset is characterized by a fixed anomaly or 'scar', while symptom remission or persistence is associated with brain maturation and normalization, or compensation and reorganization.[9] The trajectories of remission and persistence from childhood through adulthood occur in parallel to or in interaction with other neurodevelopmental processes (e.g. development of executive functions).The development of frontal and temporal areas engaged in emotional and cognitive processes does not plateau until adulthood, which coincides with the typical

bioRxiv preprint doi: https://doi.org/10.1101/2020.09.24.311654; this version posted September 25, 2020. The copyright holder for this preprint (which was not certified by peer review) is the author/funder. All rights reserved. No reuse allowed without permission.

age range of ADHD symptom remission.[1,10] Maturation in these regions may compensate for the initial childhood development of ADHD symptoms through top-down regulatory processes, leading to eventual symptom remission.[8] Therefore, longitudinal cohort studies are essential to dissect the upstream, parallel, or downstream brain mechanisms in reference to symptom remission. Compared to a cross-sectional approach, a longitudinal design provides not only unique insights into the temporal dynamics of underlying biological processes, but also increased statistical power by reducing between-subject variability.[11,12]

Neurodevelopmental mechanisms underlying the variable long-term course of ADHD may be partly traceable using neuroimaging. Healthy brain development has been characterized using structural and functional magnetic resonance imaging (MRI), showing trajectories across the lifespan of regional volumes and activity/connectivity, respectively.[13–15] Those that have applied diffusion, magnetization transfer, relaxometry, and myelin water imaging methods have also demonstrated consistent, rapid white matter (WM) microstructural changes in the first three years of life, reflecting increased myelination or axonal packing.[10] These changes continue throughout adolescence and are associated with corresponding age-related changes in gray matter.[16] However, regarding later childhood and adolescence, the paucity of congruous findings in other WM imaging modalities besides diffusion weighted imaging (DWI) suggests that changes are primarily related to myelination and axonal packing.[10] With age, WM increases in overall volume, becoming more myelinated in a region-specific fashion and reaching peak values later in life.[17,18] The rate of development differs between WM regions, progressing in an outward, central-to-peripheral direction, wherein sensory and motor regions generally mature the earliest.

bioRxiv preprint doi: https://doi.org/10.1101/2020.09.24.311654; this version posted September 25, 2020. The copyright holder for this preprint (which was not certified by peer review) is the author/funder. All rights reserved. No reuse allowed without permission.

DWI studies have revealed WM microstructural abnormalities in ADHD, specifically using fractional anisotropy (FA), which is the metric we focus on here.[4,5,9,19–22] DWI reveals information about anatomical connectivity in the brain *in vivo* by measuring the directionality of water diffusion in WM tracts, thus enabling inferences about underlying brain mechanisms by quantifying associated changes in (inter)cellular space.[20,23] FA is an indirect measure of microstructural integrity—sensitive to myelination, parallel organization and fiber bundle density.[24] A systematic meta-analysis of case-control DWI studies in ADHD found that lower FA in ADHD has mostly been reported in interhemispheric, frontal and temporal regions—however, higher FA has also been found in similar areas.[4] Given these previous WM associations with ADHD and the brain's maturation in those same areas during an age range typical for symptom remission, the next step is to determine how WM microstructural alterations coincide with remission versus persistence of ADHD symptoms over time.

Not many longitudinal studies have examined the neurobiological underpinnings of symptom remission in WM—and none have longitudinally applied DWI. While there are no previous studies with longitudinal DWI measurements, there have been some clinical longitudinal studies with one DWI measurement. A follow-up DWI analysis three decades after diagnosis supports the theory of the disorder as an enduring neurobiological trait independent of remission; both remittent and persistent probands with an ADHD diagnosis in childhood had widespread reduced FA compared to those who did not have childhood ADHD.[25] Conversely, a network connectivity analysis of two clinical assessments and one resting-state functional MRI measurement at follow-up pointed to the presence of compensatory mechanisms that aid symptomatic remission in prefrontal regions and the executive control network: higher connectivity at follow-up was associated with HI decreases.[22] A study performed with a sample overlapping with the current study (but at an earlier sampling time

bioRxiv preprint doi: https://doi.org/10.1101/2020.09.24.311654; this version posted September 25, 2020. The copyright holder for this preprint (which was not certified by peer review) is the author/funder. All rights reserved. No reuse allowed without permission.

with mean age 11.9-17.8 years) found, somewhat counterintuitively, that more HI symptom remission was associated with lower FA in the left corticospinal tract (lCST) and left superior longitudinal fasciculus (lSLF) at follow-up.[7] This previous study included clinical data from two time-points and only one DWI time-point.

Our current investigation is a continuation of our earlier DWI work in this cohort, and extends upon it in three ways. First, by capturing an older age range, we have a more complete picture of symptom remission (mean age range: 16.91-20.57 years; Figure 1 is a schematic of how our study chronologically relates to that of Francx *et al.*[7]). Second, DWI measurements at two time-points allow for a more thorough investigation of the chronology and mechanisms of FA development in relation to symptom remission. Third, we used Permutation Analysis of Linear Models (PALM), a newly available permutation-based analysis technique, to account for the family structure in our sample.[26,27] We aimed to examine whether symptom remission may be underpinned by WM alterations as adolescents with ADHD develop into adulthood. Given our longitudinal DWI data, we were able to distinguish between (1) pre-existing WM features that predict the likelihood of symptoms to remit or persist, (2) WM changes over time that occur concurrently with symptom change, and (3) WM alterations that may be a (direct or indirect) downstream consequence of symptom remission versus persistence.

bioRxiv preprint doi: https://doi.org/10.1101/2020.09.24.311654; this version posted September 25, 2020. The copyright holder for this preprint (which was not certified by peer review) is the author/funder. All rights reserved. No reuse allowed without permission.

Methods

Participants

Clinical and MRI data were collected in two waves from probands with childhood ADHD, their first-degree relatives, and healthy families: NeuroIMAGE1 (TP1) and NeuroIMAGE2 (TP2).[28–30] The current study included probands, affected and unaffected siblings, and healthy controls who participated in both TP1 and TP2 studies and had DWI data available from both waves (N=120). Individuals diagnosed with autism, epilepsy, general learning difficulties, known genetic disorders, brain disorders, or IQ<70 at either time point were excluded. After exclusion based on incidental findings, head motion (framewise displacement), visual artefacts in the DWI data, and outliers in global FA, the final sample consisted of 99 participants from 65 families. For both groups, there were no differences between the participants included in the current analysis and the complete sample on measures of ADHD severity, age, and sex (P>0.05). We normalized head motion z-scores after excluding outliers. Global FA at TP1, TP2, and the difference between TP1 and TP2 were normally distributed. Our sample's demographic and clinical characteristics are shown in Table 1.

Clinical measurements

Conners Parent Rating Scale (CPRS) questionnaires were used to assess the severity of 27 inattention (IA) and hyperactive-impulsive (HI) symptoms at TP1 and TP2.[31] We chose to use CPRS instead of the self-rated report because it was the consistent measure across waves and ages. We used raw CPRS scores to increase the distribution width, and analyzed HI, IA, and combined symptom scores per subject, per time point. Here, we define symptom change as the score difference: $\Delta CPRS = CPRS_{TP1} - CPRS_{TP2}$. Thus, a more positive Δ value indicates more symptom improvement.

bioRxiv preprint doi: https://doi.org/10.1101/2020.09.24.311654; this version posted September 25, 2020. The copyright holder for this preprint (which was not certified by peer review) is the author/funder. All rights reserved. No reuse allowed without permission.

Data acquisition and DWI pre-processing

MRI data were acquired with a 1.5-Tesla AVANTO scanner (Siemens, Erlangen, Germany). The scanner was equipped with an 8-channel receive-only phased-array head coil. Whole-brain diffusion-weighted images were collected (twice refocused pulsed-gradient spin-echo EPI; 60 diffusion-weighted directions spanning an entire sphere; b-value 1000 s/mm^2; 5 non-diffusion weighted images; interleaved slice acquisition; TE/TR=97/8500 ms; GRAPPA-acceleration factor 2; no partial Fourier; voxel size 2x2x2.2 mm). DWI acquisition parameters are described in detail elsewhere.[29]

To minimize movement during acquisition, all participants had tape on their heads, were asked to keep still, and received feedback when they moved too much. During pre-processing, DWI images were realigned and corrected for residual eddy current and for artefacts from head and/or cardiac motion using robust tensor modelling (PATCH).[32] We qualitatively inspected DWI data and excluded subjects whose data were of insufficient quality with strong distortions or artifacts beyond correction with our processing protocol (N=4). Diffusion tensor characteristics and FA values were calculated for each voxel.[33]

Longitudinal TBSS

We performed whole brain voxel-wise analyses with Tract-Based Spatial Statistics (TBSS).[34] Our study's longitudinal design called for an analysis pipeline that considered how within-subject changes may be greater than between-subject changes; intra-subject data alignment across time brings extra difficulty compared to cross-subject nonlinear registration to common space.[12,35] Within-subject longitudinal differences may even be removed when different nonlinear warps are used for the same brain at multiple time points. Consequently,

bioRxiv preprint doi: https://doi.org/10.1101/2020.09.24.311654; this version posted September 25, 2020. The copyright holder for this preprint (which was not certified by peer review) is the author/funder. All rights reserved. No reuse allowed without permission.

we used a bespoke pipeline adapted from others to create a non-biased individual subject template.[12,35] Figure 2 summarizes our TBSS pipeline which includes the following steps:

1. Images were initially registered (FLIRT) with an appropriate optimization schedule validated for longitudinal studies.[36,37] Volumes from both time points were resampled into the space halfway between the two, which required only a single registration per volume and minimized registration bias towards one of the time points.[38]
2. Both halfway-registered FA maps were averaged to generate a subject-wise mid-space template (i.e. base FA template).
3. To smoothen the base FA templates, we added extra mode-dilation and erosion, which prevented inflation in zero-value voxels and the disruption of the resultant FA skeleton, yielding an improved, better-connected FA skeleton.
4. TBSS was used to non-linearly register the base FA template of each subject automatically to FMRIB58 FA standard-space.
5. The mean FA image was created and thinned into a mean FA skeleton, representing the centers of all tracts common to the sample.
6. The skeleton was thresholded at FA>0.20 and binarized to suppress areas of low mean FA and/or high inter-subject variability.
7. Each subject's aligned FA data from both time-points was projected onto the skeleton.
8. Voxel-wise difference in FA was calculated by subtracting the 4D skeletonized FA images of TP1 from those of TP2 ($\Delta FA = FA_{TP2} - FA_{TP1}$). A more positive ΔFA value indicates the development of more anisotropic (i.e. directional) diffusion over time, while a more negative ΔFA value indicates the development of more isotropic diffusion over time.

bioRxiv preprint doi: https://doi.org/10.1101/2020.09.24.311654; this version posted September 25, 2020. The copyright holder for this preprint (which was not certified by peer review) is the author/funder. All rights reserved. No reuse allowed without permission.

Statistical analysis

We constructed three general linear models for our voxel-wise analyses (Table S1): We kept difference in raw total CPRS score (ΔCPRS) as a constant predictor, while separately testing FA at baseline (TP1), follow-up (TP2), and the difference between TP1 and TP2 (ΔFA) as dependent variables (models 1, 2, and 3, respectively). Our main analyses first examined combined symptom scores and, if significant, subsequent analyses examined whether effects were driven by HI or IA. Fixed effects included sex, normalized head motion (framewise displacement) at respective time point(s), age at TP1, age difference between TP1 and TP2, and CPRS symptom score at TP1 (Figure 1, Table S1, Figure S2). We used PALM to account for the lack of independence in the data due to sibling relationships and shared variance between families, constraining permutation tests between families of the same sizes.[26] We designed multi-level exchangeability blocks which did not allow permutation among all individuals; permutations were constrained both at the whole-block level (i.e. permute between families of the same size) and the within-block level (i.e. permute within families) (Figure S1). We corrected for multiple testing by running 5000 permutations and threshold-free cluster enhancement (TFCE) as implemented in PALM, part of the FSL toolbox (https://fsl.fmrib.ox.ac.uk/fsl/fslwiki/PALM).[26,27,39] Results with TFCE-corrected $P<0.05$ were considered statistically significant. All tests used the standard parameter settings for height, extent, and connectivity: H=2, E=1, C=26. We used the Johns Hopkins University DTI-based WM atlas in FSL to relate any significant clusters to known WM tracts.[40]

bioRxiv preprint doi: https://doi.org/10.1101/2020.09.24.311654; this version posted September 25, 2020. The copyright holder for this preprint (which was not certified by peer review) is the author/funder. All rights reserved. No reuse allowed without permission.

Results

Symptom change over time

In Table 1, we present mean symptom scores for HI, IA, and combined (HI+IA). Combined symptom scores significantly decreased over time ($t(98)=4.884$, $P_{FWE}=2.027\times10^{-6}$). This was due to decreases in both IA scores ($t(98)=4.226$, $P_{FWE}=2.672\times10^{-5}$) and HI scores ($t(98)=4.394$, $P_{FWE}=1.410\times10^{-5}$), with a mean decrease of 2.04 (SD=4.80) in IA, and 1.46 (SD=3.30) in HI score.

Symptom change in relation to WM microstructure at two time-points

There was no significant association between combined symptom score remission and FA at TP1, but a negative association between combined symptom score remission and FA at TP2 was observed in two clusters: lSLF ($P_{FWE}=0.038$) and lCST ($P_{FWE}=0.044$) (Table 2A; Figure 4A). This was mainly driven by a negative effect of HI dimension score on FA in lCST ($P_{FWE}=0.049$; Table 2B; Figure 4B).

Additionally, there was a negative trend association between combined symptom score difference and FA difference ($P=0.079$). Because our one model with a significant effect, as well as those previously reported in an overlapping sample at an earlier time window, were driven by HI, we performed an exploratory *post-hoc* analysis on symptom score difference and FA difference with only HI dimension scores.[5,7] More HI symptom remission was associated with a larger decrease in FA over time in ten clusters spread over six WM tracts (Table 2C).

bioRxiv preprint doi: https://doi.org/10.1101/2020.09.24.311654; this version posted September 25, 2020. The copyright holder for this preprint (which was not certified by peer review) is the author/funder. All rights reserved. No reuse allowed without permission.

Post hoc tests of confounders and demographics

Sex, normalized head motion at respective time point(s), age at TP1, age difference between TP1 and TP2, and CPRS symptom score at TP1 were included as covariates in all models. We report main effects after the removal of non-significant interaction effects (Table 2). We found neither a significant main effect of any of these variables, nor an interaction effect of any of these variables with ΔCPRS for all analyses reported above (Table S2).

bioRxiv preprint doi: https://doi.org/10.1101/2020.09.24.311654; this version posted September 25, 2020. The copyright holder for this preprint (which was not certified by peer review) is the author/funder. All rights reserved. No reuse allowed without permission.

Discussion

In this longitudinal investigation of ADHD and WM microstructure, we report that more symptom remission is associated with lower FA at follow-up in lCST and lSLF, an effect mainly driven by HI symptom remission. Thereby, we have essentially replicated and extended the findings reported by Francx et al. (2015) at an older age range, contributing to the growing body of evidence describing the progression of ADHD and its relation with WM. Additionally, we utilized an improved statistical method to account for the family structure in our data, thus confirming that previous results in this cohort were not confounded by within-family correlations.[7,27] By substantiating those earlier findings, with replication in participants at an older age, and upon better accounting for family relatedness, we conclude that symptom remission from early adolescence is associated with lower FA in late adolescence and young adulthood.

Our longitudinal design of two diagnostic and two DWI time-points allows us to speculate about the chronology of brain changes versus symptom changes. First, we found no evidence that baseline FA predicts ADHD symptom change over time. Second, though a natural expectation would be that more remission leads to higher FA, we found the opposite, somewhat paradoxical result: More ADHD symptom remission was associated with lower FA at follow-up in lSLF and lCST. Third, we found that HI, rather than IA, symptom remission was the main driver behind the association with reduced FA in lCST. WM microstructure can change in response to behavior or learning (i.e. plasticity).[35] It is possible that decreased (motor) hyperactivity is associated with less use of corticospinal and motor tracts, which may lead to decreased FA in this area at TP2. Overall, lower FA in both tracts appears to follow, rather than precede, symptom remission. Speculatively, this suggests that

bioRxiv preprint doi: https://doi.org/10.1101/2020.09.24.311654; this version posted September 25, 2020. The copyright holder for this preprint (which was not certified by peer review) is the author/funder. All rights reserved. No reuse allowed without permission.

the WM changes may be a downstream result, rather than a cause, of symptom remission in ADHD.

FA is an indirect reflection of microstructure and some neuronal processes that improve anatomical connectivity may paradoxically manifest as decreased FA in some locations—especially in principal WM highways through which several fibers cross, like the SLF and CST. At the axonal level, more sprouting, pruning, crossing fibers or fiber dispersion in those tracts during maturation may demonstrate as reduced FA over time. Plasticity in myelin or axon integrity in less dominant fibers could also exhibit as reduced FA in voxels containing multiple fiber orientations. In our participants whose symptoms persisted, higher FA could be the outcome of brain reorganization in less dominant fiber tracts, particularly in those that traverse the CST and SLF. Event-related and resting-state functional MRI studies that grouped their subjects categorically have reported that remitters have stronger connectivity than persisters.[22,41] Lower functional connectivity in certain tracts may be related to higher FA in other tracts and vice versa. In a top-down fashion, remitters may learn compensatory strategies to overcome their ADHD symptoms as they age, while persisters may either learn disadvantageous strategies, other beneficial compensatory strategies, or none at all, leading to divergent trajectories of WM development in various brain regions in individuals with persistent ADHD symptoms.[42]

One can find in the literature several instances wherein the SLF and CST are implicated in ADHD. The SLF generally subserves a wide variety of functions related to language, attention, memory, emotion, and visuospatial function; many studies have pointed to its function in visuospatial awareness, as well as attentional selection of sensory content.[21,43,44] Our findings are partly in accordance with those of others that have found

bioRxiv preprint doi: https://doi.org/10.1101/2020.09.24.311654; this version posted September 25, 2020. The copyright holder for this preprint (which was not certified by peer review) is the author/funder. All rights reserved. No reuse allowed without permission.

neurodevelopmental effects linked with unilaterally compromised lSLF maturation during adolescence.[45] Thus, ADHD symptom persistence may influence higher unilateral SLF integrity as a person develops from early adolescence to young adulthood. The CST integrates cortical and lower brain processing centers in the motor system, has an important role in modulating sensory information, and may be particularly relevant to motor hyperactivity in ADHD.[46] Altered modulation of sensory information could potentially be involved in HI remission, as the CST contains fibers running from the primary motor, premotor, supplementary motor, somatosensory, parietal and cingulate cortex to the spine and is thus involved in the control of complex voluntary distal movements.[47] Correspondingly, the persistence of HI could, indeed, result in increased FA in CST through time. Our unilateral findings may have risen from the fact that 88% of our subjects were right-handed, and most CST axons cross to the contralateral side at the pyramidal decussation before reaching lower motor neurons.[47] We found no evidence that handedness was correlated with change in symptom scores (Table S3).

Based on previous investigations that have similarly found effects of ADHD symptoms on WM microstructure driven by HI, we also conducted an exploratory analysis of only HI symptom remission effects on change in FA.[5,7,20] Our results suggest that HI symptom remission is associated with more decrease in FA over time. Most of the associations we found were clustered in prefrontal and frontostriatal regions. Higher functional connectivity in prefrontal networks in young adults has been associated with more improvement in symptoms over time.[7,41] Likewise, the prefrontal cortex and its connections are especially important in the remission or persistence of ADHD symptoms.[8,22] As it continues to develop throughout adolescence, the prefrontal cortex can potentially compensate for the initial causes of ADHD through its connectivity with subcortical regions such as the striatum.

bioRxiv preprint doi: https://doi.org/10.1101/2020.09.24.311654; this version posted September 25, 2020. The copyright holder for this preprint (which was not certified by peer review) is the author/funder. All rights reserved. No reuse allowed without permission.

Indeed, a study using independent component analysis demonstrated that ADHD diagnosis was significantly associated with reduced brain volume in a component that mapped to the frontal lobes, the striatum, and their interconnecting WM tracts.[48] Although exploratory and tentative, our finding of decreased FA in frontostriatal regions coinciding with HI symptom remission is thus in line with Halperin & Schulz's theory: Neural plasticity and the development of the prefrontal cortex and interconnected neural circuits facilitate recovery over the course of development.[8]

We used a dimensional approach in defining the ADHD phenotype, in line with our recent findings in a large overlapping cohort wherein no evidence was found for altered FA in association with categorical ADHD diagnosis.[5] Unaffected participants clustered at the low end of the score distribution. Given the relatively small number of fully remitted patients (N=5), together with a subset of 'partly remitted' individuals, our use of symptom severity as a continuous variable maximized power to detect symptom-related changes, while also circumventing arbitrary decisions on the definition of remission.[49] We thus interpret our findings in terms of symptom severity, reflecting the degree of remission in ADHD patients as well as variation in individuals who do not reach diagnostic threshold.

Head motion is quite typical in the ADHD population and is hence a common confound in such studies.[4,19,32,50] A previous meta-analysis of DWI studies in ADHD found that most investigations that controlled for head motion did not have significant results.[4] We normalized head motion and included it as a confound covariate in all of our analyses, as well as checked each model for an interaction effect with the head motion parameter. We found no evidence that it had an influence on our results.

bioRxiv preprint doi: https://doi.org/10.1101/2020.09.24.311654; this version posted September 25, 2020. The copyright holder for this preprint (which was not certified by peer review) is the author/funder. All rights reserved. No reuse allowed without permission.

FA estimates can be less accurate in brain regions consisting of so-called "kissing" and/or crossing fibers, like the CST and SLF. FA gives only one value for the overall restriction of anisotropy in a voxel, which could be a crucial aspect in the inconsistency of findings in the literature regarding WM and ADHD. Future studies may include complementary longitudinal region-of-interest tractography analyses in the clusters that we found to be significant, or by using DWI methods that deliver greater resolution at the neurite level. Techniques that utilize orientation dispersion indices or WM fiber density could potentially provide clarity in the constant discourse of how crossing fibers can mar inferences about FA and brain effects of ADHD. Likewise, incorporating additional DWI data from more than two time points throughout development would, naturally, increase statistical power and enhance our understanding of the dynamic interplay between disorder and development.

Conclusion

We used two DWI time-points in a longitudinal study of dimensional symptom scores in ADHD. Our results indicate that, in specific WM tracts, greater symptom improvement results in lower FA at follow-up. We show that WM alterations may occur downstream of symptom change. The effects we have found confirm and extend earlier findings in an overlapping sample; they indicate divergent trajectories of WM development in individuals with persistent ADHD symptoms compared to those showing remittance, and support the role of prefrontal and sensorimotor development in the remission of ADHD.

bioRxiv preprint doi: https://doi.org/10.1101/2020.09.24.311654; this version posted September 25, 2020. The copyright holder for this preprint (which was not certified by peer review) is the author/funder. All rights reserved. No reuse allowed without permission.

References

1. Faraone S V, Asherson P, Banaschewski T, et al. Attention-deficit/hyperactivity disorder. *Nat Rev Dis Prim*. 2015;1:15020. http://eutils.ncbi.nlm.nih.gov/entrez/eutils/elink.fcgi?dbfrom=pubmed&id=27189265&retmode=ref&cmd=prlinks.
2. American Psychiatric Association. *American Psychiatric Association, 2013. Diagnostic and Statistical Manual of Mental Disorders (5th Ed.)*.; 2013. doi:10.1176/appi.books.9780890425596.744053
3. Hoogman M, Bralten J, Hibar DP, et al. Subcortical brain volume differences in participants with attention deficit hyperactivity disorder in children and adults: a cross-sectional mega-analysis. *The Lancet Psychiatry*. 2017;4(4):310-319. doi:10.1016/S2215-0366(17)30049-4
4. Aoki Y, Cortese S, Castellanos FX. Research Review: Diffusion tensor imaging studies of attention-deficit/hyperactivity disorder: meta-analyses and reflections on head motion. *J Child Psychol Psychiatry Allied Discip*. 2018;59(3):193-202. doi:10.1111/jcpp.12778
5. Damatac CG, Chauvin RJM, Zwiers MP, et al. White matter microstructure in attention-deficit/hyperactivity disorder: a systematic tractography study in 654 individuals. *Biol Psychiatry Cogn Neurosci Neuroimaging*. August 2020:787713. doi:10.1016/j.bpsc.2020.07.015
6. Franke B, Michelini G, Asherson P, et al. Live fast , die young ? A review on the developmental trajectories of ADHD across the lifespan. *Eur Neuropsychopharmacol*. 2018;28(10):1059-1088. doi:10.1016/j.euroneuro.2018.08.001
7. Francx W, Zwiers MP, Mennes M, et al. White matter microstructure and developmental improvement of hyperactive/impulsive symptoms in attention-

bioRxiv preprint doi: https://doi.org/10.1101/2020.09.24.311654; this version posted September 25, 2020. The copyright holder for this preprint (which was not certified by peer review) is the author/funder. All rights reserved. No reuse allowed without permission.

deficit/hyperactivity disorder. *J Child Psychol Psychiatry Allied Discip*. 2015;56(12):1289-1297. doi:10.1111/jcpp.12379

8. Halperin JM, Schulz KP. Revisiting the role of the prefrontal cortex in the pathophysiology of attention-deficit/hyperactivity disorder. *Psychol Bull*. 2006;132(4):560-581. doi:10.1037/0033-2909.132.4.560
9. Sudre G, Mangalmurti A, Shaw P. Growing out of attention deficit hyperactivity disorder: Insights from the 'remitted' brain. *Neurosci Biobehav Rev*. 2018;94(September):198-209. doi:10.1016/j.neubiorev.2018.08.010
10. Lebel C, Deoni S. The development of brain white matter microstructure. *Neuroimage*. 2018;182(3):207-218. doi:10.1016/j.neuroimage.2017.12.097
11. Thompson WK, Hallmayer J, O'Hara R. Design Considerations for Characterizing Psychiatric Trajectories Across the Lifespan: Application to Effects of APOE-ε4 on Cerebral Cortical Thickness in Alzheimer's Disease. *Am J Psychiatry*. 2011;168(9):894-903. doi:10.1176/appi.ajp.2011.10111690
12. Madhyastha T, Mérillat S, Hirsiger S, et al. Longitudinal reliability of tract-based spatial statistics in diffusion tensor imaging. *Hum Brain Mapp*. 2014;35(9):4544-4555. doi:10.1002/hbm.22493
13. Brouwer RM, Klein M, Grasby KL, et al. Dynamics of Brain Structure and its Genetic Architecture over the Lifespan. *bioRxiv*. 2020. doi:10.1101/2020.04.24.031138
14. Brouwer RM, Hedman AM, van Haren NEM, et al. Heritability of brain volume change and its relation to intelligence. *Neuroimage*. 2014. doi:10.1016/j.neuroimage.2014.04.072
15. van Duijvenvoorde ACK, Westhoff B, de Vos F, Wierenga LM, Crone EA. A three-wave longitudinal study of subcortical–cortical resting-state connectivity in adolescence: Testing age- and puberty-related changes. *Hum Brain Mapp*.

bioRxiv preprint doi: https://doi.org/10.1101/2020.09.24.311654; this version posted September 25, 2020. The copyright holder for this preprint (which was not certified by peer review) is the author/funder. All rights reserved. No reuse allowed without permission.

2019;40(13):3769-3783. doi:10.1002/hbm.24630

16. Giorgio A, Watkins KE, Douaud G, et al. Changes in white matter microstructure during adolescence. *Neuroimage*. 2008;39(1):52-61. doi:10.1016/j.neuroimage.2007.07.043

17. Paus T, Collins DL, Evans AC, Leonard G, Pike B, Zijdenbos A. Maturation of white matter in the human brain: A review of magnetic resonance studies. *Brain Res Bull*. 2001;54(3):255-266. doi:10.1016/S0361-9230(00)00434-2

18. Kochunov P, Williamson DE, Lancaster J, et al. Fractional anisotropy of water diffusion in cerebral white matter across the lifespan. *Neurobiol Aging*. 2012;33(1):9-20. doi:10.1016/j.neurobiolaging.2010.01.014

19. van Ewijk H, Heslenfeld DJ, Zwiers MP, Buitelaar JK, Oosterlaan J. Diffusion tensor imaging in attention deficit/hyperactivity disorder: A systematic review and meta-analysis. *Neurosci Biobehav Rev*. 2012;36(4):1093-1106. doi:10.1016/j.neubiorev.2012.01.003

20. van Ewijk H, Heslenfeld DJ, Zwiers MP, et al. Different mechanisms of white matter abnormalities in attention-deficit/ hyperactivity disorder: A diffusion tensor imaging study. *J Am Acad Child Adolesc Psychiatry*. 2014;53(7):790-799.e3. doi:10.1016/j.jaac.2014.05.001

21. Shaw P, Sudre G, Wharton A, Weingart D, Sharp W, Sarlls J. White matter microstructure and the variable adult outcome of childhood attention deficit hyperactivity disorder. *Neuropsychopharmacology*. 2015;40(3):746-754. doi:10.1038/npp.2014.241

22. Francx W, Oldehinkel M, Oosterlaan J, et al. The executive control network and symptomatic improvement in attention-deficit / hyperactivity disorder. *Cortex*. 2015;73:62-72. doi:j.cortex.2015.08.012

bioRxiv preprint doi: https://doi.org/10.1101/2020.09.24.311654; this version posted September 25, 2020. The copyright holder for this preprint (which was not certified by peer review) is the author/funder. All rights reserved. No reuse allowed without permission.

23. Beaulieu C. The basis of anisotropic water diffusion in the nervous system - A technical review. *NMR Biomed*. 2002;15(7-8):435-455. doi:10.1002/nbm.782

24. Chang EH, Argyelan M, Aggarwal M, et al. The role of myelination in measures of white matter integrity: Combination of diffusion tensor imaging and two-photon microscopy of CLARITY intact brains. *Neuroimage*. 2017;147(3):253-261. doi:10.1016/j.neuroimage.2016.11.068

25. Cortese S, Imperati D, Zhou J, et al. White matter alterations at 33-year follow-up in adults with childhood attention-deficit/hyperactivity disorder. *Biol Psychiatry*. 2013;74(8):591-598. doi:10.1016/j.biopsych.2013.02.025

26. Winkler AM, Ridgway GR, Webster MA, Smith SM, Nichols TE. Permutation inference for the general linear model. *Neuroimage*. 2014;92:381-397. doi:10.1016/j.neuroimage.2014.01.060

27. Winkler AM, Webster MA, Vidaurre D, Nichols TE, Smith SM. Multi-level block permutation. *Neuroimage*. 2015;123:253-268. doi:10.1016/j.neuroimage.2015.05.092

28. Müller UC, Asherson P, Banaschewski T, et al. The impact of study design and diagnostic approach in a large multi-centre ADHD study. Part 1: ADHD symptom patterns. *BMC Psychiatry*. 2011;11(1):54. doi:10.1186/1471-244X-11-54

29. von Rhein D, Mennes M, van Ewijk H, et al. The NeuroIMAGE study: a prospective phenotypic, cognitive, genetic and MRI study in children with attention-deficit/hyperactivity disorder. Design and descriptives. *Eur Child Adolesc Psychiatry*. 2015;24(3):265-281. doi:10.1007/s00787-014-0573-4

30. Müller UC, Asherson P, Banaschewski T, et al. The impact of study design and diagnostic approach in a large multi-centre ADHD study: Part 2: Dimensional measures of psychopathology and intelligence. *BMC Psychiatry*. 2011;11(1):55. doi:10.1186/1471-244X-11-55

bioRxiv preprint doi: https://doi.org/10.1101/2020.09.24.311654; this version posted September 25, 2020. The copyright holder for this preprint (which was not certified by peer review) is the author/funder. All rights reserved. No reuse allowed without permission.

31. Conners CK, Erhardt D, Epstein JN, Parker JDA, Sitarenios G, Sparrow E. Self-ratings of ADHD symptoms in adults I: Factor structure and normative data. *J Atten Disord*. 1999. doi:10.1177/108705479900300303

32. Zwiers MP. NeuroImage Patching cardiac and head motion artefacts in diffusion-weighted images. *Neuroimage*. 2010;53(2):565-575. doi:10.1016/j.neuroimage.2010.06.014

33. Behrens TEJJ, Woolrich MW, Jenkinson M, et al. Characterization and Propagation of Uncertainty in Diffusion-Weighted MR Imaging. *Magn Reson Med*. 2003;50(5):1077-1088. doi:10.1002/mrm.10609

34. Smith SM, Jenkinson M, Johansen-berg H, et al. Tract-based spatial statistics: Voxelwise analysis of multi-subject diffusion data. *Neuroimage*. 2006;31(4):1487-1505. doi:10.1016/j.neuroimage.2006.02.024

35. Engvig A, Fjell AM, Westlye LT, et al. Memory training impacts short-term changes in aging white matter: A Longitudinal Diffusion Tensor Imaging Study. *Hum Brain Mapp*. 2012;33(10):2390-2406. doi:10.1002/hbm.21370

36. Smith SM, Rao A, De Stefano N, et al. Longitudinal and cross-sectional analysis of atrophy in Alzheimer's disease: Cross-validation of BSI, SIENA and SIENAX. *Neuroimage*. 2007;36(4):1200-1206. doi:10.1016/j.neuroimage.2007.04.035

37. Jenkinson M, Smith S. A global optimisation method for robust affine registration of brain images. *Med Image Anal*. 2001;5(2):143-156. doi:10.1016/S1361-8415(01)00036-6

38. Smith SM, De Stefano N, Jenkinson M, Matthews PM. Normalized accurate measurement of longitudinal brain change. *J Comput Assist Tomogr*. 2001;25(3):466-475. doi:10.1097/00004728-200105000-00022

39. Smith SM, Nichols TE. Threshold-free cluster enhancement: Addressing problems of

bioRxiv preprint doi: https://doi.org/10.1101/2020.09.24.311654; this version posted September 25, 2020. The copyright holder for this preprint (which was not certified by peer review) is the author/funder. All rights reserved. No reuse allowed without permission.

smoothing, threshold dependence and localisation in cluster inference. *Neuroimage*. 2009;44(1):83-98. doi:10.1016/j.neuroimage.2008.03.061

40. Hua K, Zhang J, Wakana S, et al. Tract probability maps in stereotaxic spaces: Analyses of white matter anatomy and tract-specific quantification. *Neuroimage*. 2008;39(1):336-347. doi:10.1016/j.neuroimage.2007.07.053

41. Clerkin SM, Schulz KP, Berwid OG, et al. Thalamo-cortical activation and connectivity during response preparation in adults with persistent and remitted ADHD. *Am J Psychiatry*. 2013;170(9):1011-1019. doi:10.1176/appi.ajp.2013.12070880

42. Wetterling F, Mccarthy H, Tozzi L, et al. Impaired reward processing in the human prefrontal cortex distinguishes between persistent and remittent attention deficit hyperactivity disorder. *Hum Brain Mapp*. 2015;36(11):4648-4663. doi:10.1002/hbm.22944

43. Conner AK, Briggs RG, Rahimi M, et al. A Connectomic Atlas of the Human Cerebrum—Chapter 10: Tractographic Description of the Superior Longitudinal Fasciculus. *Oper Neurosurg*. 2018;15(suppl_1):S407-S422. doi:10.1093/ons/opy264

44. Wolfers T, Onnink AMH, Zwiers MP, et al. Lower white matter microstructure in the superior longitudinal fasciculus is associated with increased response time variability in adults with attentiondeficit/hyperactivity disorder. *J Psychiatry Neurosci*. 2015;40(5):344-351. doi:10.1503/jpn.140154

45. Peters BD, Szeszko PR, Radua J, et al. White matter development in adolescence: Diffusion tensor imaging and meta-analytic results. *Schizophr Bull*. 2012;38(6):1308-1317. doi:10.1093/schbul/sbs054

46. Moreno-López Y, Olivares-Moreno R, Cordero-Erausquin M, Rojas-Piloni G. Sensorimotor integration by corticospinal system. *Front Neuroanat*. 2016;10(MAR):1-6. doi:10.3389/fnana.2016.00024

bioRxiv preprint doi: https://doi.org/10.1101/2020.09.24.311654; this version posted September 25, 2020. The copyright holder for this preprint (which was not certified by peer review) is the author/funder. All rights reserved. No reuse allowed without permission.

47. Welniarz Q, Dusart I, Roze E. The corticospinal tract: Evolution, development, and human disorders. *Dev Neurobiol*. 2017;77(7):810-829. doi:10.1002/dneu.22455

48. Cupertino RB, Soheili-Nezhad S, Grevet EH, et al. Reduced fronto-striatal volume in ADHD in two cohorts across the lifespan. *bioRxiv*. 2019. doi:10.1101/790204

49. Du Rietz E, Cheung CHM, McLoughlin G, et al. Self-report of ADHD shows limited agreement with objective markers of persistence and remittance. *J Psychiatr Res*. 2016. doi:10.1016/j.jpsychires.2016.07.020

50. Yendiki A, Koldewyn K, Kakunoori S, Kanwisher N, Fischl B. Spurious group differences due to head motion in a diffusion MRI study. *Neuroimage*. 2014;88(88):79-90. doi:10.1016/j.neuroimage.2013.11.027

bioRxiv preprint doi: https://doi.org/10.1101/2020.09.24.311654; this version posted September 25, 2020. The copyright holder for this preprint (which was not certified by peer review) is the author/funder. All rights reserved. No reuse allowed without permission.

Figures and Tables

	TP1		TP2			
	Mean	**(SD)**	**Mean**	**(SD)**	**Test Statistic**	**(*P*)**
Age	16.91	(3.47)	20.57	(3.52)		
Sex (female)	N = 42	42%	N = 42	42%		
Estimated IQ	105.15	(15.02)	106.44	(16.38)	F(1,100) = 0.84	(0.38)
Head motion	0.51	(0.35)	0.47	(0.22)	F(1,100) = 2.41	($<10^{-4}$)
Handedness (right)	N = 89	89%	N = 89	89%		
CPRS by group						
Combined	12.76	(12.11)	9.26	(10.20)		
Affected	24.38	(9.63)	18.86	(10.03)		
Subthreshold	8.55	(7.79)	7.13	(7.55)		
Unaffected	4.04	(4.40)	3.06	(4.07)		
Inattention	8.05	(7.65)	6.02	(6.65)		
Affected	15.05	(5.98)	12.17	(6.55)		
Subthreshold	5.64	(5.35)	4.53	(4.44)		
Unaffected	2.76	(3.82)	2.06	(3.14)		
Hyperactivity-impulsivity	4.71	(5.30)	3.25	(4.23)		
Affected	9.32	(5.28)	6.69	(4.88)		
Subthreshold	2.91	(3.05)	2.60	(3.20)		
Unaffected	1.28	(1.64)	1.00	(1.65)		
Medication use						
Duration (days)	669	(1050)	1184	(1742)		
Ever used (yes)	N = 46	46%	N = 46	46%		

bioRxiv preprint doi: https://doi.org/10.1101/2020.09.24.311654; this version posted September 25, 2020. The copyright holder for this preprint (which was not certified by peer review) is the author/funder. All rights reserved. No reuse allowed without permission.

Table 1. Demographic and clinical characteristics of the sample at NeuroIMAGE1 (TP1) and NeuroIMAGE2 (TP2) with mean and standard deviation. Demographic between-group differences were tested using F-tests for continuous variables and $\chi 2$-tests for categorical variables. Reported values pertain to all participants who were included in the final sample after all quality control (N=99). IQ was estimated at both timepoints using the vocabulary and block design subtests of the Wechsler Intelligence Scale for Children (WISC-III) or Wechsler Adult Intelligence Scale (WAIS-III). Combined CPRS symptom score is the sum of two separate dimensions: hyperactivity-impulsivity and inattention. Medications: Ritalin (methylphenidate), Concerta (methylphenidate), Strattera (atomoxetine), and any other ADHD medication. The majority of patients were taking prescription medication for ADHD, mostly methylphenidate or atomoxetine. Duration of medication use was recorded on the day of MRI scan as the cumulative number of days of use, while the history of medication use was recorded as whether or not the participant had ever taken ADHD medication.

bioRxiv preprint doi: https://doi.org/10.1101/2020.09.24.311654; this version posted September 25, 2020. The copyright holder for this preprint (which was not certified by peer review) is the author/funder. All rights reserved. No reuse allowed without permission.

	Model	WM tract	N_{voxels}	MNI (Peak voxel) X_{COG}	Y_{COG}	Z_{COG}	t_{max}	P_{FWE}
A.	$FA_{TP2} \sim \Delta CPRS_{combined}$	lCST	723	-21	-27	44	0.755	0.044
		lSLF	579	-33	-20	38	0.881	0.038
B.	$FA_{TP2} \sim \Delta CPRS_{HI}$	lCST	17	-18	-25	52	0.981	0.049
C.	$\Delta FA \sim \Delta CPRS_{HI}$	lIFOF	508	-29	24	17	0.441	0.041
		lIFOF	376	-17	31	-10	0.613	0.035
		Fmin	339	-18	50	0	0.585	0.042
		lUNC	174	-25	17	-8	0.564	0.045
		lCST	158	-22	-13	8	0.562	0.047
		Fmin	22	-20	38	21	0.563	0.049
		CCG	17	-17	32	23	0.562	0.049
		lIFOF	11	-28	15	-1	0.563	0.049
		Fmin	11	-18	46	17	0.566	0.049
		Fmin	9	-12	41	-17	0.563	0.049

Table 2. TBSS results: WM tracts, peak voxels, and localization of significant clusters (P_{FWE}<0.05) clusters of voxel-wise permutation based dimensional analyses (PALM) in models 2 and 3. N_{voxels}: number of voxels, $X/Y/Z_{COG}$: location of the center of gravity for the cluster (vox/mm), MNI: Montreal Neurological Institute, t_{max}: highest TFCE t-statistic value per cluster, WM: white matter, lCST: left corticospinal tract, lSLF: left superior longitudinal fasciculus, lIFOF: left inferior fronto-occipital fasciculus, Fmin: forceps minor of the corpus callosum, lUNC: left uncinate fasciculus, CCG: cingulum cingulate gyrus.

A. Model 2: Less combined symptom remission was associated with more FA at follow-up in lSLF and lCST.
B. Model 2 *post-hoc*: Negative effect in model 2 was driven by HI score remission.
C. Model 3 *post-hoc*: More HI symptom remission was associated with a larger decrease in FA over time in several WM clusters.

bioRxiv preprint doi: https://doi.org/10.1101/2020.09.24.311654; this version posted September 25, 2020. The copyright holder for this preprint (which was not certified by peer review) is the author/funder. All rights reserved. No reuse allowed without permission.

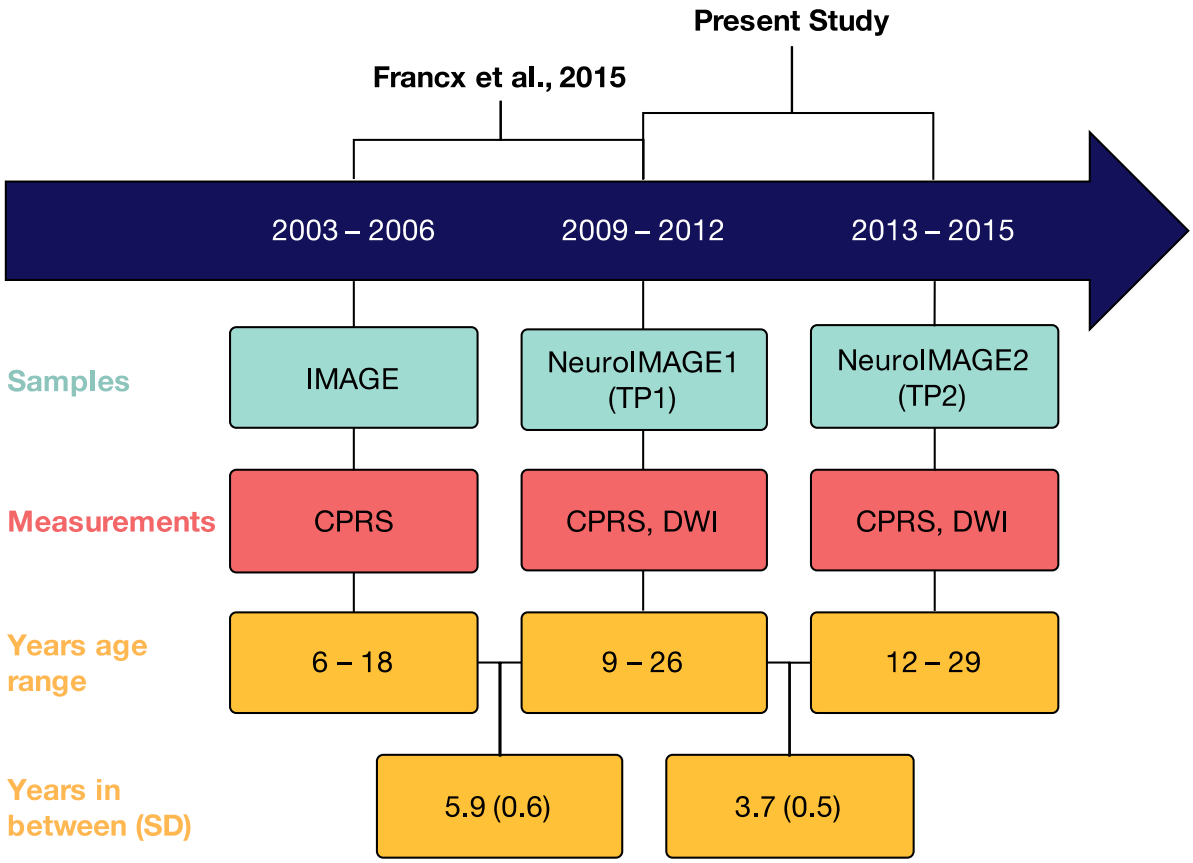

Figure 1. Schematic diagram of how this study chronologically relates to that of Francx et al. (2015), as well as the study samples included, relevant clinical and imaging measurements, study sample age ranges, and mean years (with standard deviation) in between each measurement time point.[7,29,30] The present study is an analysis of TP1 and TP2. DWI: diffusion-weighted imaging, CPRS: Conners Parent Rating Scale.[31]

bioRxiv preprint doi: https://doi.org/10.1101/2020.09.24.311654; this version posted September 25, 2020. The copyright holder for this preprint (which was not certified by peer review) is the author/funder. All rights reserved. No reuse allowed without permission.

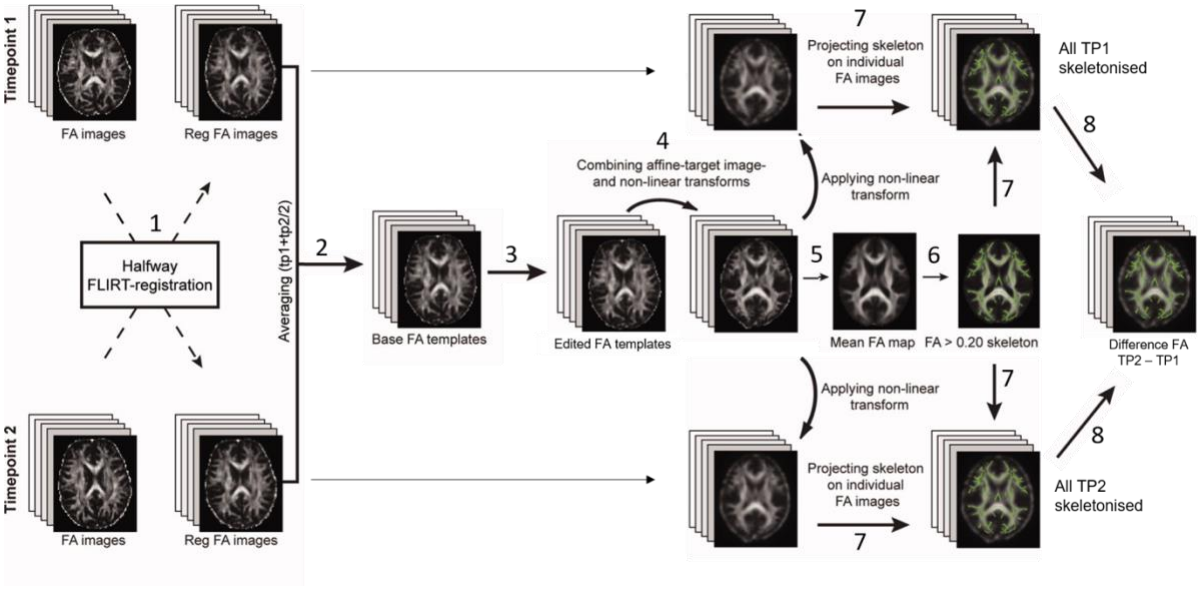

Figure 2. Our longitudinal TBSS pipeline was adapted to create a nonbiased individual subject template for use as a base template (2), which was then non-linearly registered to FMRIB58 FA standard-space (4) to create a mean FA skeleton (5), onto which each subject's aligned FA data from both time points was projected (7).

bioRxiv preprint doi: https://doi.org/10.1101/2020.09.24.311654; this version posted September 25, 2020. The copyright holder for this preprint (which was not certified by peer review) is the author/funder. All rights reserved. No reuse allowed without permission.

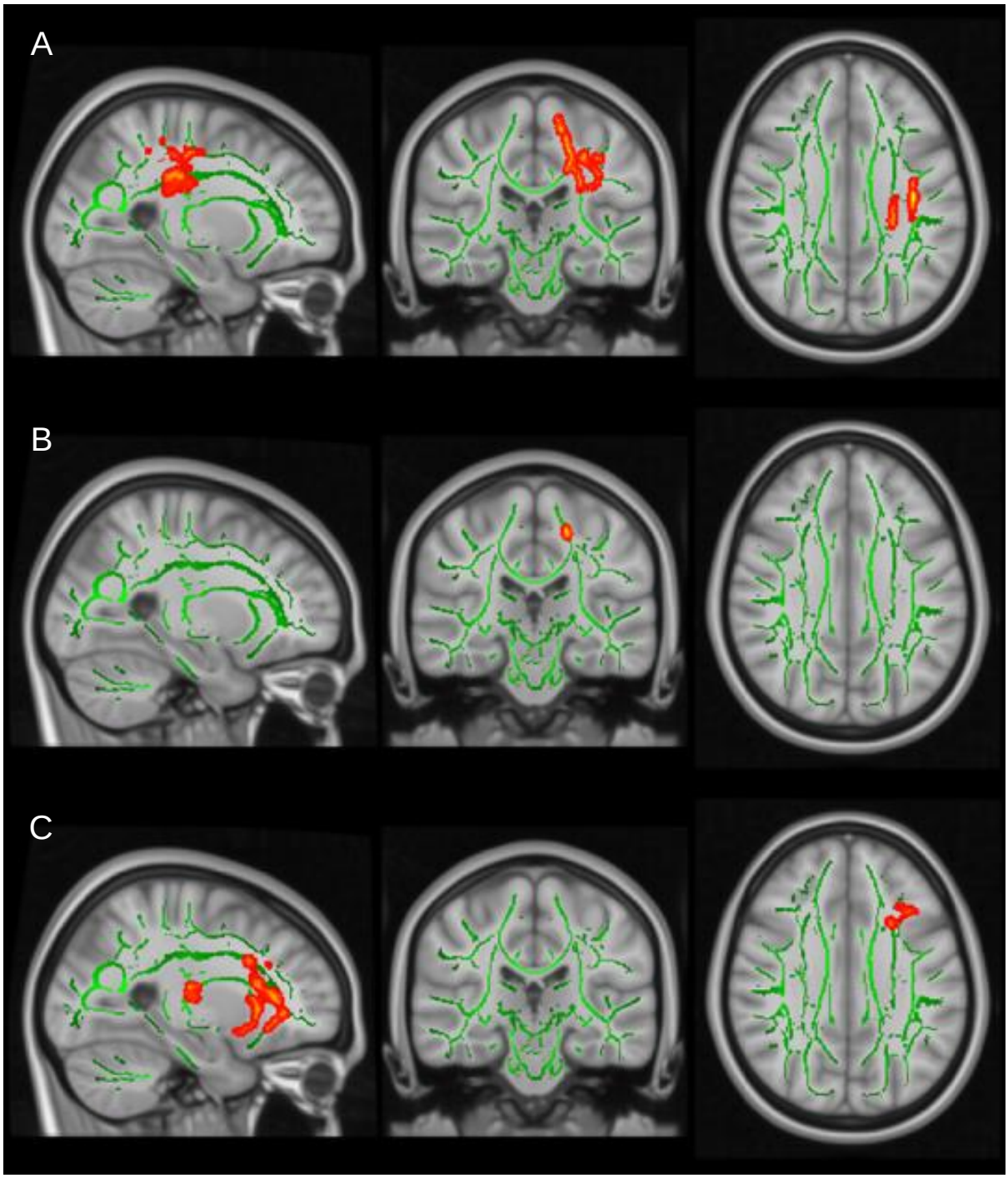

Figure 3. Dimensional TBSS analyses showing significant associations (red-yellow) between FA values and the CPRS scores over time. The mean FA skeleton across all subjects (green) was overlain on the MNI template image for presentation (x=-25, y=-25, z=31). Results were thickened for visualization (FSL "tbss_fill") and presented here in radiological convention from sagittal, coronal, and axial perspectives, respectively.

A. Lower FA values at follow-up (TP2) were associated with a larger decrease in combined symptom score in the left superior longitudinal fasciculus (lSLF) (P_{FWE}=0.038) and the left corticospinal tract (lCST) (P_{FWE}=0.044).
B. Lower FA values at TP2 were associated with a larger decrease in HI symptom score in lCST (P_{FWE}=0.049).
C. A more negative change in FA (i.e. more isotropic diffusion) over time was associated with more HI symptom remission in ten clusters spread over six WM tracts. See Table 2 for cluster statistics and locations.

bioRxiv preprint doi: https://doi.org/10.1101/2020.09.24.311654; this version posted September 25, 2020. The copyright holder for this preprint (which was not certified by peer review) is the author/funder. All rights reserved. No reuse allowed without permission.

Supplementary material

Model 1	FA_{TP1}	~	ΔCPRS	+	age_{TP1}	+	Δage	+	sex	+	$CPRS_{TP1}$	+	head $motion_{TP1}$		
Model 2	FA_{TP2}	~	ΔCPRS	+	age_{TP1}	+	Δage	+	sex	+	$CPRS_{TP2}$	+	head $motion_{TP2}$		
Model 3	ΔFA	~	ΔCPRS	+	age_{TP1}	+	Δage	+	sex	+	$CPRS_{TP1}$	+	head $motion_{TP1}$	+	head $motion_{TP2}$

Table S1. The composition of our three different models. We essentially have a cross-lagged design with FA as the dependent variable. Models 1, 2 and 3 all have the difference in CPRS ($\Delta CPRS = CPRS_{TP1} - CPRS_{TP2}$) as the predictor variable. The outcome variables of these models are, respectively: FA at TP1, FA at TP2, and change in FA. Our use of PALM necessitated that we kept the (TBSS output) FA image as the dependent variable.

			MNI (Peak voxel)					
Model	**WM tract**	**N_{voxels}**	**X_{COG}**	**Y_{COG}**	**Z_{COG}**	***t_{max}***	***P_{FWE}***	**age_{TP1} interaction *P***
$FA_{TP2} \sim \Delta CPRS_{combined}$	lCST	723	-21	-27	44	0.755	0.044	0.463
	lSLF	579	-33	-20	38	0.881	0.038	0.808
$FA_{TP2} \sim \Delta CPRS_{HI}$	lCST	17	-18	-25	52	0.981	0.049	0.154
$\Delta FA \sim \Delta CPRS_{HI}$	lIFOF	508	-29	24	17	0.441	0.041	0.667
	lIFOF	376	-17	31	-10	0.613	0.035	0.055
	Fmin	339	-18	50	0	0.585	0.042	0.874
	lUNC	174	-25	17	-8	0.564	0.045	0.131
	lCST	158	-22	-13	8	0.562	0.047	0.130
	Fmin	22	-20	38	21	0.563	0.049	0.239
	CCG	17	-17	32	23	0.562	0.049	0.238
	lIFOF	11	-28	15	-1	0.563	0.049	0.238
	Fmin	11	-18	46	17	0.566	0.049	0.239
	Fmin	9	-12	41	-17	0.563	0.049	0.237

Table S2. Interaction effects of ΔCPRS and age at TP1 for significant models.

bioRxiv preprint doi: https://doi.org/10.1101/2020.09.24.311654; this version posted September 25, 2020. The copyright holder for this preprint (which was not certified by peer review) is the author/funder. All rights reserved. No reuse allowed without permission.

ΔCPRS score	**Spearman's ρ**	***P***
Combined	0.038	0.709
Hyperactivity-impulsivity	0.098	0.331
Inattention	-0.007	0.948

Table S3. Correlation (Spearman's rho) between difference in CPRS score ($\Delta CPRS = CPRS_{TP1} - CPRS_{TP2}$) and right-handedness in our sample.

bioRxiv preprint doi: https://doi.org/10.1101/2020.09.24.311654; this version posted September 25, 2020. The copyright holder for this preprint (which was not certified by peer review) is the author/funder. All rights reserved. No reuse allowed without permission.

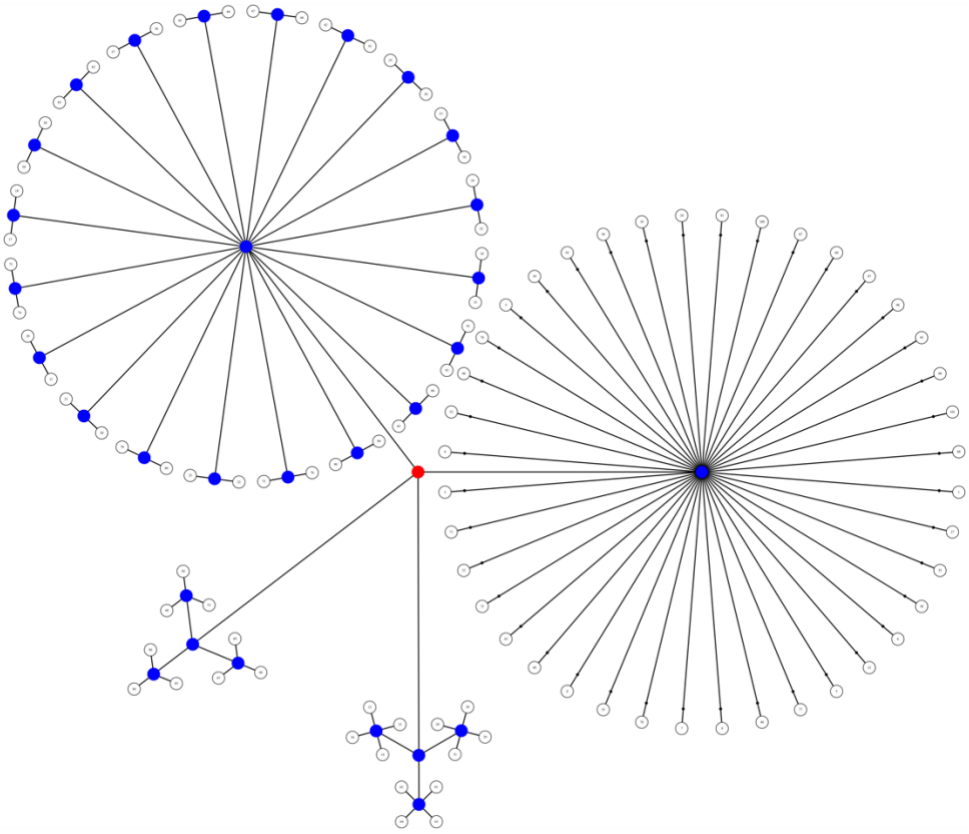

Figure S1. Visual representation of the multi-level notation of family structure in our sample. The four groups represent the size of each family: 3 families of 3 children, 3 families of 4 children, 20 families of 2 children, and 40 families of 1 child in the study. We depict the levels as branches from the central red node, akin to a tree in which the most peripheral elements (leaves) represent the observations. The nodes from which the branches depart either allow (blue) or do not allow (red) permutations.

bioRxiv preprint doi: https://doi.org/10.1101/2020.09.24.311654; this version posted September 25, 2020. The copyright holder for this preprint (which was not certified by peer review) is the author/funder. All rights reserved. No reuse allowed without permission.

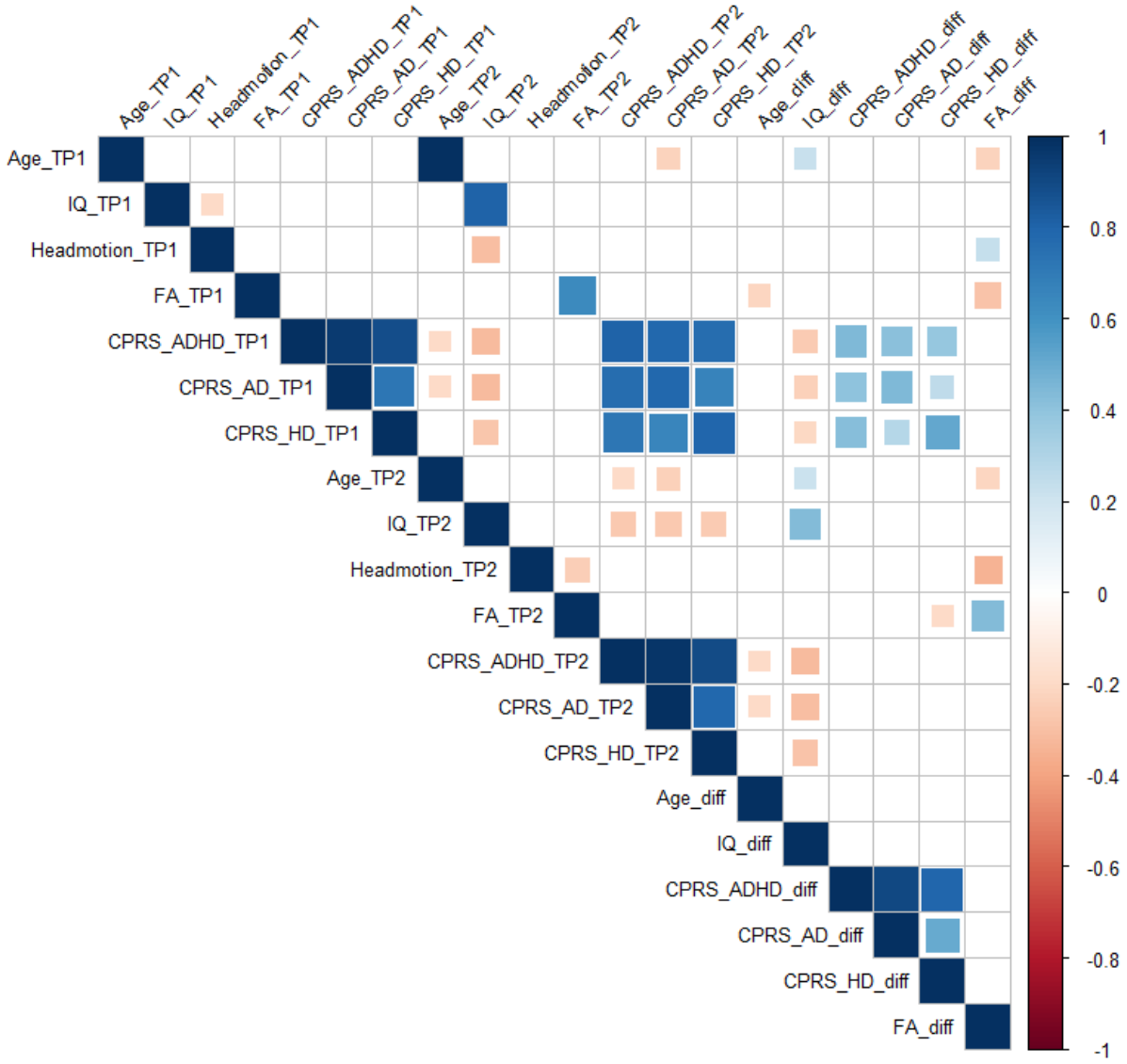

Figure S2. Spearman correlation matrix of independent and dependent variables, as well as covariates. These correlation tests were performed before the main analyses. The color intensity of each box indicates the magnitude of the correlation. Positive correlations are presented in blue and negative correlations in red. The size of the box indicates its significance, with significant correlations filling each square completely.